

A quantitative assessment of the 1998 carbon monoxide emission anomaly in the Northern Hemisphere based on total column and surface concentration measurements

L. N. Yurganov,¹ T. Blumenstock,² E. I. Grechko,³ F. Hase,² E. J. Hyer,⁴ E. S. Kasischke,⁴ M. Koike,⁵ Y. Kondo,⁵ I. Kramer,² F.-Y. Leung,⁶ E. Mahieu,⁷ J. Mellqvist,⁸ J. Notholt,^{9,10} P. C. Novelli,¹¹ C. P. Rinsland,¹² H. E. Scheel,¹³ A. Schulz,⁹ A. Strandberg,⁸ R. Sussmann,¹³ H. Tanimoto,¹⁴ V. Velazco,¹⁵ R. Zander,⁷ and Y. Zhao¹⁶

Received 22 January 2004; revised 14 May 2004; accepted 3 June 2004; published 6 August 2004.

[1] Carbon monoxide abundances in the atmosphere have been measured between January 1996 and December 2001 in the high Northern Hemisphere (HNH) (30°–90°N) using two different approaches: total column amounts of CO retrieved from infrared solar spectra and CO mixing ratios measured in situ at ground-based stations. The data were averaged, and anomalies of the CO HNH burden (deviations of the total tropospheric mass between 30°N and 90°N from the mean seasonal profile, determined as the 5 year average) were analyzed. The anomalies obtained from in situ and total column data agree well and both show two maxima, by far the largest in October 1998 and a lower one in August 1996. A noticeable decrease of the positive 1998 summer anomaly with increasing height was found. A box model was applied, and anomalies in source rates were obtained under the assumption of insignificant interannual sink variations. In August 1998 the HNH emission anomaly was estimated to be 38 Tg month⁻¹. The annual 1998 emission positive anomaly was 96 Tg yr⁻¹. Nearly all excess CO may be attributed to the emissions from boreal forest fires. According to available inventories, biomass burning emits around 52 Tg yr⁻¹ during the “normal” years; therefore total biomass emissions in 1998 were as large as 148 Tg yr⁻¹. In August 1998, CO contribution from the biomass burning was twice as large as that from fossil fuel combustion. The results were compared to available emission inventories. *INDEX TERMS*: 0365 Atmospheric Composition and Structure: Troposphere—composition and chemistry; 0368 Atmospheric Composition and Structure: Troposphere—constituent transport and chemistry; 1610 Global Change: Atmosphere (0315, 0325); *KEYWORDS*: carbon monoxide, forest fires, spectroscopy

1. Introduction

[2] Carbon monoxide (CO) is a chemically active trace gas with a lifetime that varies from 10 days over summer continental regions to well over a year at the winter poles

[Holloway *et al.*, 2000]. It is a by-product of most combustion. According to Holloway *et al.* [2000], during a normal year (without catastrophic wild fires), biomass burning contributes 748 Tg CO yr⁻¹ (or 690 Tg CO yr⁻¹, according to Andreae and Merlet [2001]) to the global budget of CO. Therefore biomass burning provides a larger source of CO than that of fossil fuel (300 Tg yr⁻¹), and its contribution is

¹Frontier Research System for Global Change, Japan Agency for Marine-Earth Science and Technology, Yokohama, Japan.

²Institute of Meteorology and Climate Research, Forschungszentrum Karlsruhe, Karlsruhe, Germany.

³Obukhov Institute of Atmospheric Physics, Moscow, Russia.

⁴Department of Geography, University of Maryland, College Park, Maryland, USA.

⁵University of Tokyo, Tokyo, Japan.

⁶Division of Engineering and Applied Sciences, Department of Earth and Planetary Sciences, Harvard University, Cambridge, Massachusetts, USA.

⁷Institute of Astrophysics and Geophysics, University of Liège, Liège, Belgium.

⁸Radio and Space Science, Chalmers University of Technology, Göteborg, Sweden.

⁹Alfred-Wegener-Institute, Potsdam, Germany.

¹⁰Now at University of Bremen, Bremen, Germany.

¹¹Climate Monitoring and Diagnostic Laboratory, NOAA, Boulder, Colorado, USA.

¹²Atmospheric Sciences Division, NASA Langley Research Center, Hampton, Virginia, USA.

¹³Institute of Meteorology and Climate Research, Forschungszentrum Karlsruhe, Garmisch-Partenkirchen, Germany.

¹⁴National Institute for Environmental Studies, Tsukuba, Japan.

¹⁵University of Bremen, Bremen, Germany.

¹⁶University of California, Davis, California, USA.

comparable with those from the oxidation of biogenic hydrocarbons (683 Tg yr^{-1}) or from the methane oxidation (760 Tg yr^{-1}). *Ehhalt et al.* [2001] adopted $1550 \text{ Tg CO yr}^{-1}$ directly emitted to the atmosphere from Earth's surface. This value includes biomass burning emission, $700 \text{ Tg CO yr}^{-1}$, and fossil and domestic fuel emission, $650 \text{ Tg CO yr}^{-1}$. In situ chemical oxidation of various hydrocarbons is adopted for that report as $1230 \text{ Tg CO yr}^{-1}$ (including 800 Tg CO from the oxidation of methane). Total sources of CO were estimated by *Ehhalt et al.* [2001] as $2780 \text{ Tg CO yr}^{-1}$.

[3] A reaction with hydroxyl (OH) is responsible for 90–95% of the CO removal from the atmosphere [*Logan et al.*, 1981; *Holloway et al.*, 2000]. CO in turn destroys OH, accounting for 30–60% of OH loss [*Spivakovsky et al.*, 2000]. OH is known to be an important atmospheric “detergent” with highly variable low concentrations. Variations of the CO concentration influence OH concentrations and modify the oxidation and thus the cleansing capacity of the atmosphere.

[4] CO is the second most abundant gas (after carbon dioxide CO_2) emitted by biomass burning; according to *Andreae and Merlet* [2001], extratropical forest fires account for 68 Tg CO yr^{-1} versus $1004 \text{ Tg CO}_2 \text{ yr}^{-1}$. However, the percent perturbation of CO background burden due to wild fires is much larger than that of CO_2 because CO concentrations in the troposphere are more than three orders of magnitude lower. Biomass burning in the high Northern Hemisphere (30° – 90°N) has a high interannual variability, which can be observed through its effect on atmospheric CO concentrations.

[5] CO in the lower troposphere is monitored using surface-based sampling followed by a gas-chromatographic analysis at the Climate Monitoring and Diagnostic Laboratory (CMDL) network of NOAA [see *Novelli et al.*, 1998, 2003]. CO is measured directly at several stations of the Northern Hemisphere (NH) (e.g., at the Global Atmospheric Watch network) [*World Meteorological Organization (WMO)*, 2003]. Observational sites that are free of local contaminations are normally located on islands or at the seashore and measure CO in the marine boundary layer (MBL); continental stations are subject to various local influences, and their data are typically omitted in the analysis of global trends and other variations. Several mountain sites measure free tropospheric (FT) CO concentrations; however, in many cases, local orographic and circulation patterns result in uplifting of air from the boundary layer (BL). These data therefore require careful filtering to characterize the FT [e.g., *Rinsland et al.*, 2000]. CO concentrations in the FT are also measured sporadically during field experiments and campaigns involving aircrafts [see, e.g., *TRACE-P Science Team*, 2003].

[6] An alternative to the in situ observations is the spectroscopic technique that employs spectra of solar light absorbed by the column of air above the station. If the station is located near sea level, the retrieved CO total columns include the BL and the FT contributions. Local sources may significantly perturb concentrations near the surface, but their relative contributions to total column amounts are small. If a spectroscopic station is located high in the mountains, it then measures the partial column amount that characterizes the FT. In both cases the long

optical path of the measurement allows concentrations to be averaged over large vertical domains.

[7] Enhanced CO mixing ratios up to 180 ppb near the surface were found during some days in August 1998 at Mace Head, Ireland [*Forster et al.*, 2001]. Simulations with the particle dispersion model FLEXPART confirmed transport of CO from Canadian forest fires. However, the high observed background CO concentrations (97 ppb) could not be explained by Canadian sources alone. *Forster et al.* [2001, p. 22,903] assumed that “boreal forest fires in Canada and Russia may therefore together strongly enhance the CO background of the Northern Hemisphere.”

[8] The measurements of CO mixing ratios in the surface layer at Rishiri Island, Japan, in 1998 revealed episodic high concentrations (up to 800 ppb) and baseline enhancement from summertime to early fall [*Tanimoto et al.*, 2000]. They explained these effects by the transport of CO from boreal forest fires in Siberia.

[9] Significant CO perturbations in 1997–1998 were also detected in total column measurements above Mauna Loa, Hawaii [*Rinsland et al.*, 1999], Jungfraujoch, Switzerland, in 1998 [*Rinsland et al.*, 2000], Hokkaido, Japan, in August–October 1998 [*Zhao et al.*, 2002], and Zvenigorod, Russia, in 1998 [*Yurganov et al.*, 2002] (the data are presented in this paper as well). *Wotawa et al.* [2001] explained the interannual variations in the summertime CO concentration in the Northern Hemisphere as resulting from contributions by temperate and boreal forest fires.

[10] None of the abovementioned papers give a quantitative assessment of the CO emissions. *Novelli et al.* [2003] estimated that 225–400 Tg excess CO (CO produced above that in more typical years) was released to the troposphere globally due to fires in 1997–1998. Almost all this excess CO was emitted in the tropics and midlatitudes of the NH; little enhancement was observed in the high Southern Hemisphere. They assumed that the anomaly measured near the surface extends to $5 \pm 2 \text{ km}$ above sea level (asl) in the northern high latitudes and $7 \pm 2 \text{ km}$ asl in the tropics. More recently, *van der Werf et al.* [2004] evaluated contributions of six regions, including boreal forest belt (north of 38°N) using satellite-based estimates of fire activity, biogeochemical modeling, and an inverse analysis of the atmospheric CO mixing ratios from the CMDL network. They obtained a CO emission anomaly from northern boreal fires (referenced to the entire period 1997–2001) for 1998 of $76 \pm 6 \text{ Tg CO yr}^{-1}$.

[11] Considerable efforts have been made to quantify emissions from boreal fires using inventories of specific emission sources (E. S. Kasischke et al., Influences of boreal fire emissions on Northern Hemisphere atmospheric carbon and carbon monoxide, submitted to *Global Biogeochem. Cycles*, 2004, hereinafter referred to as Kasischke et al., submitted manuscript, 2004). However, these studies are severely limited by uncertainties in emission factors and in estimates of areas burned.

[12] In this work we discuss CO total column amounts derived from solar spectroscopic observations carried out between January 1996 and December 2001 at nine stations in the latitudinal belt between 30°N and 80°N . The nine stations were operated by eight laboratories. This combined data set shows in a consistent way the significant CO anomaly in 1998. The spectroscopic data provide insight into the vertical extent of the anomaly, information lacking

Table 1. Characteristics of Sites, Spectrometers, and Codes of Retrieval Procedures

Site	Coordinates	Altitude, m asl	Type of Spectrometer	Typical Resolution, cm ⁻¹	Typical Number of Spectra per Day	Retrieval Algorithm ^a
NyAlesund, Spitsbergen	78.92°N, 11.94°E	20	Bruker IFS 120HR	0.005	2–3	2
Kiruna, Sweden	67.84°N, 20.41°E	419	Bruker IFS 120HR	0.005	2–3	3
Harestua, Norway	60.22°N, 10.75°E	596	Bruker IFS 120M	0.005	12 ± 6	1
Zvenigorod, Russia	55.70°N, 36.80°E	200	Grating, home-made	0.18–0.23	17 ± 6	4
Zugspitze, German Alps	47.42°N, 10.98°E	2964	Bruker IFS 120HR	0.0045	4 ± 3	1
Jungfrauoch, Swiss Alps	46.55°N, 8.00°E	3580	Bruker IFS 120HR	0.0028 and 0.0044	6	1
Moshiri, Hokkaido, Japan	44.37°N, 142.27°E	280	Bruker IFS 120HR	0.0028 and 0.0035	2–8	1
Rikubetsu, Hokkaido, Japan	43.46°N, 143.77°E	370	Bruker IFS 120M	0.0035	2–8	1
Kitt Peak, USA	31.9°N, 111.6°W	2090	McMath-Pierce FTS	0.01–0.02	2–3	1

^aSee Appendix A.

in previous studies [see, e.g., *Novelli et al.*, 2003]. The column analysis was complemented by consideration of in situ surface sampling data both in the BL and at mountain sites. Inclusion of these latter data fills geographical gaps by adding data for the vast areas of the Pacific and North America. The study reveals a very consistent buildup of surface CO mixing ratios and total column amounts in the entire high Northern Hemisphere, regardless of location. All the data were used to determine the anomaly of CO total mass (or tropospheric burden) in the HNH. An estimate of the 1998 monthly emission anomaly was obtained using a box model (30°N–90°N, 0–10 km of altitude). We compare those results to available inventories and suggest probable reasons for the differences.

2. Experimental Techniques

[13] We present data obtained mostly by Fourier transform infrared (FTIR) spectrometers operated at nine sites (Appendix A and Table 1; the data of two closely located stations were merged). Eight sites (excluding Zvenigorod) are affiliated to the Network for Detection of Stratospheric Change (<http://www.ndsc.ws>).

[14] The measurement frequency depended on weather conditions and duration of clear sky, sunny daytime periods as well as on the relative fraction of observing time devoted to CO investigations versus other monitoring commitments (see Appendix A). The measurements at Rikubetsu and Moshiri, northern Japan, distant from each other by only 155 km, were combined and are reported hereafter under the name Hokkaido (to increase the number of observation days that depends on weather conditions). Observations at the Arctic and sub-Arctic stations (Ny Alesund and Kiruna, respectively) were impossible during polar night or low Sun in wintertime. The frequency of measurements at the Kitt Peak observatory was lower than for other sites. All the original column data are given as number of molecules per unit surface area above the station; no correction for atmospheric pressure was applied. For details of retrieval procedures, see Appendix A and *Hase et al.* [2004].

[15] *Rinsland et al.* [1998] estimated the random error of a single measurement as 2–3% and systematic error as 5%. However, typical standard deviations of daily means are larger (±15% [*Zhao et al.*, 2002]; ±10–12% [*Yurganov et al.*, 1999]). This variability is a result of changes in air masses with different CO concentrations. The frequency of measurements depends on the weather and other factors. This may introduce some error (up to 10–15%) if a monthly

mean is based on 1 or 2 days of measurements. Another limitation is a random and sparse location of the observational sites (e.g., two in Alps, two in Scandinavia, but no stations in the central United States, etc.). The latter shortcoming is partly compensated for by including surface data from the CMDL network and Japanese monitoring sites.

3. Results

[16] Monthly mean CO total column amounts (expressed in molecules cm⁻²) above the sites listed in Table 1 are reproduced in Figure 1 with triangles (Hokkaido stands for Moshiri and Rikubetsu combined). Solid lines in Figure 1 are the 5-year CO column averages from 1996 to 2001, but without 1998. With the exception of Kitt Peak they all reveal distinctly high CO column amounts in 1998. At some sites (especially at alpine stations) the CO positive anomaly appeared as early as November 1997, right after the biomass burning event in Indonesia [*Duncan et al.*, 2003b]. A spike in August 1998 at Hokkaido was discussed by *Zhao et al.* [2002] and attributed to direct CO transport from the east Siberian areas subjected to forest fires. This conclusion was confirmed by a comparison with measurements of CO concentrations in the surface layer at Rishiri Island (see Figure 2), trajectory analysis, and measurements of enhanced aerosol from a satellite. An insufficient number of measurements at Kitt Peak in 1998 and its southernmost location may explain the lack of evidence of the enhancement.

[17] The 1998 CO increase near Earth's surface was a hemispheric phenomenon [cf. *Wotawa et al.*, 2001; *Novelli et al.*, 2003]. The unusual input of CO resulted in a perturbation of the CO mixing ratios in the entire troposphere, i.e., throughout the boundary layer and into the free troposphere. Here we quantify the response of CO abundance to this impact, especially as a function of altitude. Analysis of the total column measurements and the partial column data at mountain stations, together with in situ sampling in the BL and in the FT, is used to assess this response.

[18] As was already described by *Novelli et al.* [2003], surface mixing ratios of CO at many sites in the NH were abnormally high in 1998. Examples of monthly means from four sites (representing European Arctic, North American, mid-Atlantic, and eastern Asian areas) are plotted in Figure 2. While all stations showed enhanced CO during fall 1998, the Rishiri station in northern Japan

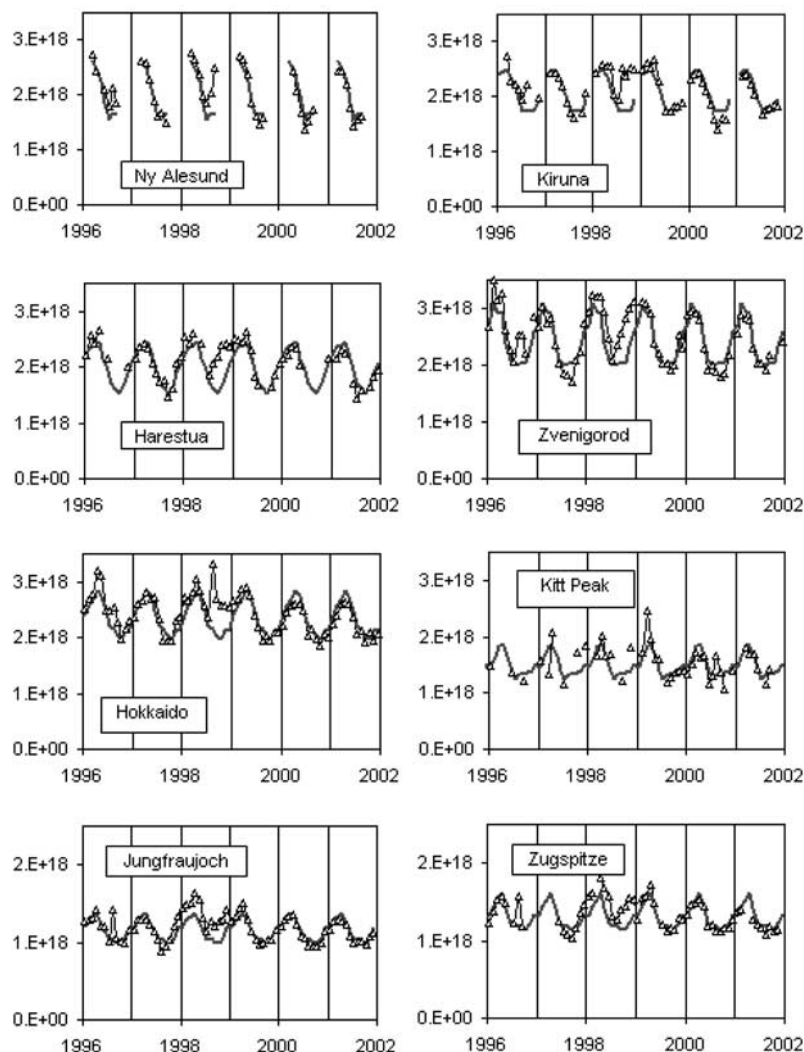


Figure 1. Monthly mean column amounts (triangles, in molecules cm^{-2}) of carbon monoxide above various sites considered in this work. Solid blue lines here and in Figure 2 correspond to the seasonal cycle, averaged over 1996, 1997, 1999, 2000, and 2001 (without 1998). See color version of this figure in the HTML.

experienced very high CO, especially in August and September 1998. *Tanimoto et al.* [2000] interpreted these increases as resulting from a direct westerly transport of CO from forest fires in eastern Siberia.

[19] All further analysis will be carried out in terms of anomalies, i.e., deviations of measured monthly values of CO abundances from those averaged between 1996 and 2001, but without 1998. This approach minimizes the influence of systematic errors introduced by retrieval techniques or differences due to geographic locations and allows the net increase in CO burden due to the changes in CO sources to be determined. Anomalies of monthly mean CO total column amounts for five low-altitude stations are plotted in Figure 3a. The curve representing data averaged over all the sites shows maxima in August 1996, in September–October 1997, and a minimum in September 1997. In fact, the 1998 anomaly was positive throughout the year, being close to $2\text{E}17$ molecules cm^{-2} during the first half and reaching the maximum of $7\text{E}17$ molecules cm^{-2} in October 1998 (almost 40% of the “normal” total

column). A “winter-spring shoulder” in the CO anomaly in January–April 1998, discussed in more detail below, cannot be explained by any emissions inside the HNH; rather, it is a result of the Indonesian fires in September–November 1997, released 130 Tg CO , according to *Duncan et al.* [2003b]. Another possible minor source of the excess CO is a transport from southern Mexico and central America, where according to *Duncan et al.* [2003a], 24 Tg CO were emitted in April–June 1998. This positive anomaly of CO total column amount lasted until the middle of 1999. The duration and the rate of this relaxation are determined by processes of CO removal, both by transport through the boundaries of the reservoir and by the chemical destruction, dominated by the reaction with hydroxyl radicals [*Holloway et al.*, 2000]. It is worth noting the exceptionally strong anomaly over Hokkaido (Moshiri and Rikubetsu) in August 1998 (up to $1.2\text{E}18$ molecules cm^{-2} , or about 60% of the average total column amount during the reference period), attributed by *Zhao et al.* [2002] to the influence of Siberian forest fires.

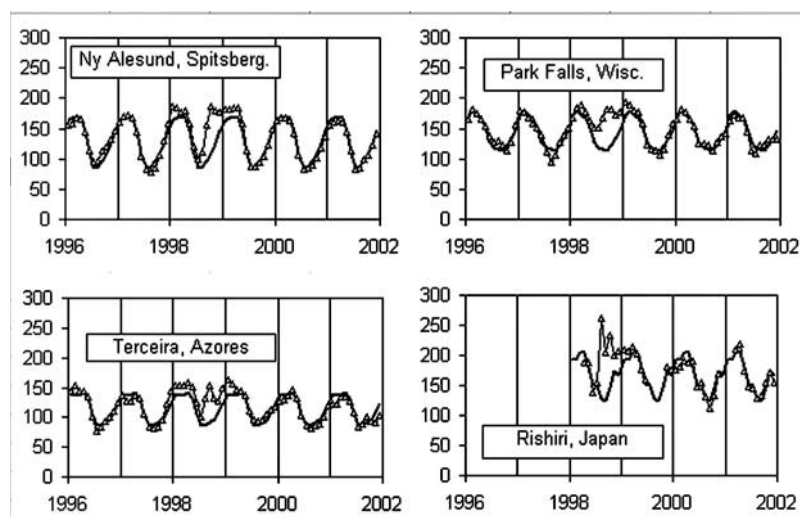


Figure 2. Examples of the CO monthly mean mixing ratios in ppb measured in the surface layer at four low-altitude sites: Ny-Alesund, Spitsbergen (colocated with the NDSC station); Park Falls, Wisconsin, USA; and Terceira, Azores (all three belong to the CMDL-NOAA network). Measurements at Rishiri Island, northern Japan, were carried out by the National Institute for Environmental Studies (NIES) and started in March 1998. See color version of this figure in the HTML.

[20] As shown in Figure 3b, CO mixing ratio anomalies observed at various stations in the BL had similar temporal shapes and absolute deviations. Again, it should be noted that the CO anomaly at Rishiri Island (150 km NW of Moshiri and 280 km NW of Rikubetsu; the sites of total column measurements, red open triangles) was 93 ppb higher than the hemispheric average anomaly in August 1998. However, the average August anomaly at Ryori station (560 km south of Moshiri, blue filled triangles) was only 28 ppb higher than the average HNH anomaly (Figure 3b). This difference cannot be explained by a different frequency of measurements and “missing” events of CO transport, as the data were recorded continuously at both sites. Thus it can be concluded that the direct effect of CO transport from the Siberian forest fires can be seen in the monthly BL mixing ratios and total column amounts only at Hokkaido (the large northern island of Japan) and its vicinity. A trajectory analysis carried out by *Zhao et al.* [2002] and by *Tanimoto et al.* [2000] confirms this conclusion. Figure 3 suggests that only part of the CO increase in the Hokkaido area (open triangles in Figure 3a) is explained by direct transport from the Siberian fires, the rest being the manifestation of the hemispheric-wide CO increase.

[21] For a quantitative analysis of the CO burden increase in the HNH reservoir, it is necessary to quantify the effect of the 1998 anomaly in the FT, keeping in mind that the BL response has already been determined by *Novelli et al.* [2003]. The column data for the two alpine stations Jungfraujoch and Zugspitze (distant by 240 km) are presented in Figure 4a along with local in situ measurements. The anomalies at these two sites agree well, and their main features are similar to those observed in other regions of the NH. The in situ CO mixing ratios measured are more scattered than the column data, but the 1998 anomalies for both techniques are mostly in the range between 20 and 40 ppb. Six in situ stations located at altitudes above 900 m

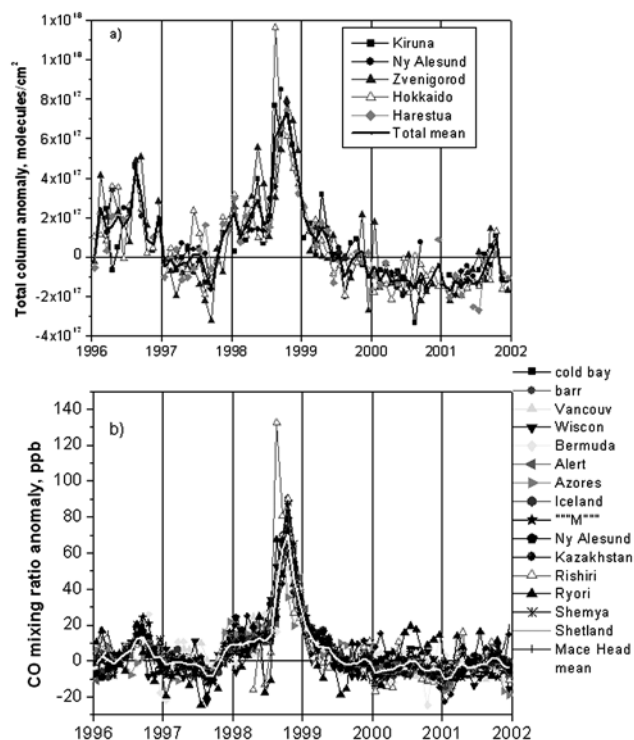


Figure 3. (a) Total column CO monthly mean anomalies (actual monthly means subtracted by the “normal” values). (b) Anomalies of the surface CO mixing ratio (see Appendix A for the geographic coordinates and affiliations). Solid curves in both plots correspond to arithmetic mean values for all sites for each month. See color version of this figure in the HTML.

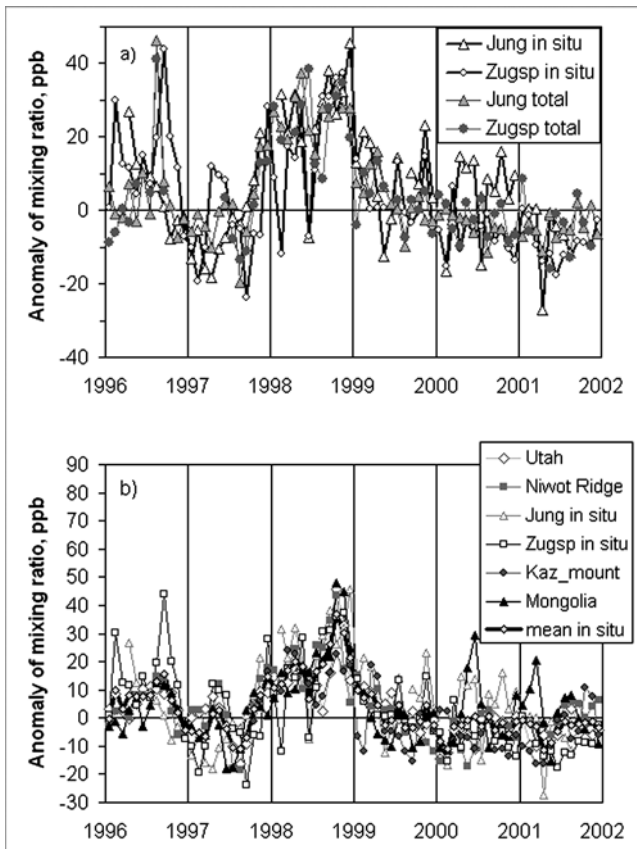


Figure 4. Monthly mean CO anomalies for high-altitude stations (with altitudes higher than 900 m asl). (a) Jungfraujoch and Zugspitze; in situ and column amount anomalies are compared. Total column amounts were divided by the total numbers of air molecules for the layer between the altitude of the station and 10 km asl (according to the 1976 U.S. Standard Atmosphere). (b) Monthly mean anomalies of CO mixing ratio, measured in situ at the mountain stations (see Appendix A for the geographic coordinates and affiliations). See color version of this figure in the HTML.

(tentatively considered as “free tropospheric” sites) also show anomalies between 20 and 40 ppb (Figure 4b). Anomalies averaged over both in situ and column measurements are used to characterize the HNH free troposphere.

[22] The anomalies were averaged over: (1) the sixteen in situ BL-located stations; (2) the six in situ mountain and two alpine column stations, taken together (FT); and (3) the five low-altitude total column stations (TC; see Figure 5). Total column CO anomalies were converted to mixing ratio anomalies in ppb dividing by the 0–10 km column numbers of air molecules above the sites (we assume that CO total column interannual variations are due to the variations of CO concentrations in the troposphere). Three domains (BL, FT, and TC) experienced a buildup, but the shapes and magnitudes were not the same. During the first half of 1998 the increase of the CO mixing ratio was higher in the free troposphere than in the BL. The HNH CO anomaly started growing as early as November 1997. According to a three-dimensional (3-D) modeling per-

formed by *Duncan et al.* [2003b], transport from the Indonesian fires affected the Northern Hemisphere through Europe, where most of the total column stations are located. It is also known that long-range transport between the hemispheres occurs mainly through the FT [e.g., *Seiler, 1974; Notholt et al., 2000*].

[23] The average in situ and column anomalies in ppb plotted in Figure 5 and the air density as a function of altitude from the 1976 U.S. Standard Atmosphere [*Minzner, 1977*] have been used for calculating the CO mass burden in each of the three reservoirs (surface area between 30°N and 90°N is 1.275E18 cm²): BL (0–1.5 km asl, air column 0.355E25 molecules cm⁻²), FT (1.5–10 km asl, 1.23E25 air molecules cm⁻²), and TC (0–10 km asl), the latter being the sum of the BL and FT burdens. The total tropospheric burden so derived from in situ and FT column measurements, together with that calculated from total column measurements of five low-altitude spectroscopic stations (Figure 3a), is plotted in Figure 6. Both curves agree very well; the 1998 annual means differ only by 3.8% (20.6 and 21.4 Tg for (FT + BL) and total column estimates). It is noteworthy that these curves are obtained using independent techniques and/or at different locations in the NH. We take the average of the two curves in Figure 6 as the most accurate estimate for the anomaly of 1998 tropospheric CO burden between 30°N and 90°N.

4. Box Model

[24] The monthly anomalies of the CO emission rate P' (Tg CO month⁻¹) in the HNH were estimated using a box model. The box had boundaries at 30°N and 90°N latitude and at 0 and 10 km altitude. P' is equal to the monthly changes of the anomalies in HNH CO burden dM'_{HNH}/dt plus anomalies of the loss L' ; the prime designates the anomaly, i.e., the deviation from the average over the

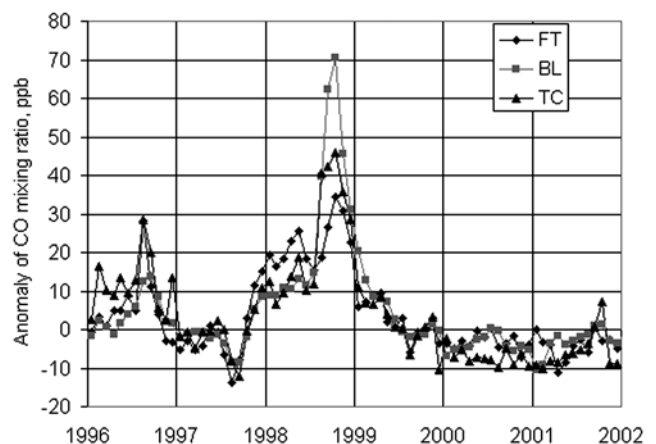


Figure 5. Average anomalies for three atmospheric domains expressed in parts per billion. Free troposphere (FT) includes data for all the mountain stations, both in situ and total column. Boundary layer (BL) comprises the low level in situ data. Total column (TC) is the average of the data for five low-level total column stations (total column amounts of CO were divided by the total numbers of air molecules). See color version of this figure in the HTML.

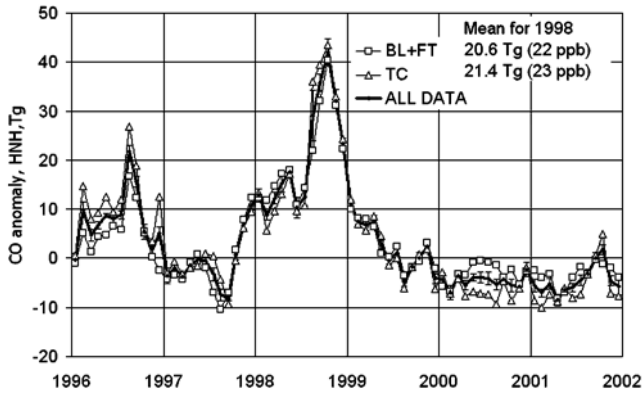


Figure 6. Monthly mean anomalies of the tropospheric CO burden (total mass between the sea level and 10 km of altitude) for the area between 30°N and 90°N. The BL + FT curve combines the data of CO sampling both at low levels and in the mountains, as well as the column data from two mountain stations. The TC curve is the average of five low-level total column stations. The “ALL DATA” curve is a simple arithmetic mean of these two curves (regardless of the number of stations). The error bars are $\text{STD} \times (N - 1)^{-1/2}$, where STD is standard deviation for individual locations and N is the number of measurement sites. See color version of this figure in the HTML.

reference period between January 1996 and December 2001, excluding 1998:

$$P' = dM'_{\text{HNH}}/dt + L'_{\text{trans}} + L'_{\text{chem}} \quad (1)$$

$$L'_{\text{trans}} = (M'_{\text{HNH}} - M'_{\text{LNH}})/\text{TAU}_{\text{trans}} \quad (2)$$

$$L'_{\text{chem}} = M'_{\text{HNH}}/\text{TAU}_{\text{chem}}. \quad (3)$$

$$\text{TAU}_{\text{chem}} = 1/k[\text{OH}], \quad (4)$$

where L'_{trans} and L'_{chem} are loss terms due to transport between the semihemispheres and OH consumption, respectively; $\text{TAU}_{\text{trans}}$ and TAU_{chem} are transport and chemical lifetimes, respectively; $[\text{OH}]$ is the hydroxyl concentration; k is the CO + OH reaction rate constant; and p is the atmospheric pressure in atm.

[25] TAU_{chem} was calculated for different atmospheric layers in the troposphere, according to equation (4), with $k = 1.5\text{E}13 (1 + 0.6 p) \text{ cm}^3 \text{ mol}^{-1} \text{ s}^{-1}$ [DeMore *et al.*, 1997] and $[\text{OH}]$ given by Spivakovsky *et al.* [2000]. Vertical pressure stratification was taken according to 1976 U.S. Standard Atmosphere [Minzner, 1977]. TAU_{chem} averaged over the box has a maximum in December (27 months), a minimum in July (1.42 months), and a mean value of 12 months for the period between November and March.

[26] A 3-D GEOS-CHEM global chemical transport model [Bey *et al.*, 2001] was used for calculations of $\text{TAU}_{\text{trans}}$. The model was driven by assimilated 1998 meteorological observations obtained from the NASA Data

Assimilation Office (DAO). The flux of CO between HNH and low Northern Hemisphere (LNH) reservoirs was calculated using a 4° (latitude) × 5° (longitude), 48 layer representation of the atmosphere. Monthly mean values of $\text{TAU}_{\text{trans}}$ were obtained as the differences in CO burdens between the semihemispheres divided by the CO flux. Annual mean of $\text{TAU}_{\text{trans}}$ was found to be 2.5 months; the summertime average was 1.5 months; and the average value for the 5-month period between November and March was 2.96 months. The interannual variations of the sink parameters were assumed to be negligible (in other words, $\text{TAU}'_{\text{chem}} = 0$ and $\text{TAU}'_{\text{trans}} = 0$); a corresponding uncertainty was estimated (see below).

[27] The $\text{TAU}_{\text{trans}}$ calculated by GEOS-CHEM was used as the most likely value. However, it was also estimated from the rate of the burden anomaly relaxation after October 1998 (Figure 7). The e -fold time (or effective lifetime) TAU_{eff} of the burden relaxation was found to be 2.34 months. The relaxation of the CO pulse in wintertime under conditions of negligible forest fire emissions was governed by both transport and chemistry, and the relation between the lifetimes may be written as [Brasseur *et al.*, 1999, p. 112]:

$$1/\text{TAU}_{\text{eff}} \approx 1/\text{TAU}_{\text{trans}} + 1/\text{TAU}_{\text{chem}}. \quad (5)$$

Using the calculated $\text{TAU}_{\text{chem}} = 12$ months and relation (5), $\text{TAU}_{\text{trans}}$ for the period November–March was estimated as 2.91 months, i.e., in good agreement with the GEOS-CHEM.

[28] The transport sink term is proportional to the difference between CO burdens in the two boxes, HNH and LNH (the latter was assumed to be bounded by latitudes 0 and 30°N, altitudes 0 and 10 km). The number of total column measurements in the LNH to estimate M'_{LNH} is insufficient; therefore we have to extend the surface measurements by Novelli *et al.* [2003] onto the entire reservoir. Model results by Taguchi *et al.* [2002] and Duncan *et al.* [2003b] indicate this may be justified; they found that a deep convection mixed emissions from the Indonesian fires well into the free troposphere with subsequent transport throughout the tropics, often as high as the tropopause.

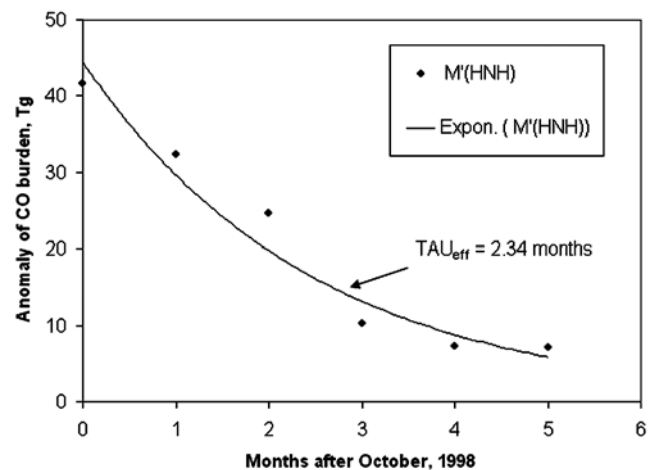


Figure 7. The exponential decay of CO anomaly after October 1998.

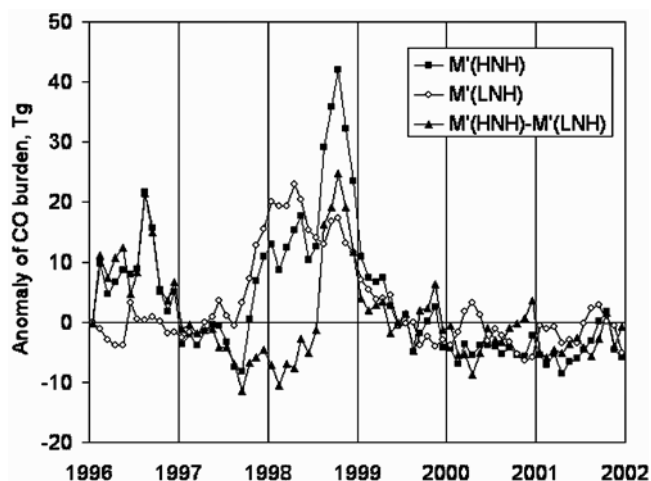


Figure 8. Anomalies of CO burden in the semihemispheres and the difference between them. See color version of this figure in the HTML.

[29] Figure 8 illustrates variations of CO burden anomalies in the two boxes and the difference between them, influencing the interbox exchange. M'_{LNH} started to grow in September 1997 in response to intense emissions from the Indonesian wild fires in September–November 1997 [Duncan *et al.*, 2003b]. M'_{HNH} followed the growth of M'_{LNH} with some delay. The CO anomaly in the LNH had a broad maximum in January–May 1998. A secondary maximum was observed in October 1998 and most probably was caused by increasing transport from the HNH (Indonesian fires stopped by that time). The difference ($M'_{HNH} - M'_{LNH}$), a “moving power” of the interbox exchange was negative during the second half of 1997 and the first half of 1998; the “winter-spring shoulder” in M'_{HNH} was caused by the influence of tropical fires on the midlatitudes of the NH. Conversely, the latitudinal gradient was positive after July 1998; the fires in the HNH in late summer of 1998 influenced the CO burden in the tropical areas of the NH during the second half of 1998.

[30] We employ several assumptions about parameters used in the box model that can influence the estimated P' . A series of calculations was performed to assess the accuracy of the P' obtained. Two options for M'_{HNH} , two options for $\text{TAU}_{\text{trans}}$, and two options for TAU_{chem} were assumed (the first options were more likely, the second options were perturbed), namely: M1, M'_{HNH} was taken as the mean of (FT + BL) and TC curves in Figure 6; M2, M'_{HNH} was taken according to the surface CMDL measurements extended to the entire box (19% higher annual 1998 anomaly and 38% higher August 1998 anomaly compared to option 1); T1, seasonally dependent $\text{TAU}_{\text{trans}}$ was calculated from GEOS-CHEM (e.g., $\text{TAU}_{\text{trans}} = 1.42$ months in July); T2, $\text{TAU}_{\text{trans}}$ was taken to be 2.9 months year-round; C1, TAU_{chem} was based on [OH] from Spivakovsky *et al.* [2000]; and C2, [OH] values of Spivakovsky *et al.* [2000] were divided by 2.

[31] P' calculated using all eight possible combinations of assumed parameters are plotted in Figure 9. The top curve corresponds to option M2 for M'_{HNH} ; option T1 for $\text{TAU}_{\text{trans}}$ and option C1 for TAU_{chem} . The bottom curve corresponds to option M1 for M'_{HNH} , option T2 for $\text{TAU}_{\text{trans}}$, and option

C2 for TAU_{chem} . The thick line and triangles correspond to the average for the eight runs; standard deviation is around $\pm(20-40)\%$ of the P' values in summertime. Rectangles are for the standard case (options M1, T1, and C1 for the parameters used).

[32] We realize that [OH] may be decreasing with increasing [CO] in 1998. Several attempts have been made to calculate this dependence. For example, Daniel and Solomon [1998] estimated that a 1% increase in CO led to a 0.34% decrease in OH for the background northern midlatitudes conditions. If this is correct, 50% increase of CO, observed in August 1998, should diminish [OH] by 17%. However, we do not use this estimate for our standard case; a change of [OH] may be larger, owing to increased concentrations of other gases over burning areas, or less, owing to possible increase of ozone, which is a source of OH. A sensitivity of emission anomaly to [OH] may be estimated from calculations with 2 times lower [OH] (Figure 9; curve “[OH]/2”); P' in August 1998 was 22% lower in comparison with the standard case.

[33] The monthly rates of excess emissions determined from the measurements using the box model (“top-down,” TD) estimates) are plotted in Figure 10. The emission anomaly was close to zero between early 1999 and late 2001. Significant positive perturbations were observed in 1996 and 1998. Negative anomalies of the emission were observed in summertime of 1997. Annual anomalies and emissions obtained from the atmospheric measurements using the box model are presented in Table 2 (the emission rates are calculated as the anomaly added to the normal emission 52 Tg CO yr^{-1}). We see that during 4 years of 6, biomass burning emissions in HNH were between 15 and

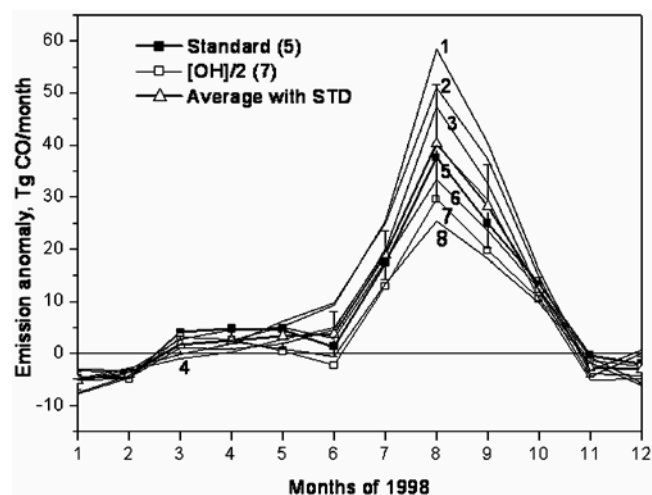


Figure 9. A study of the sensitivity of the calculated emission anomaly to the parameters of the box model. Full rectangles correspond to the standard set of parameters (M1, T1, and C1; see text); open rectangles are for the case that differs from the previous one by 2 times lower [OH] (options M1, T1, and C2). The numbers correspond to the combinations of parameters: 1 (M2, T1, and C1); 2 (M2, T2, and C1); 3 (M2, T1, and C2); 4 (M2, T2, and C2); 5 (M1, T1, and C1); 6 (M1, T2, and C1); 7 (M1, T1, and C2); 8 (M1, T2, and C2). See color version of this figure in the HTML.

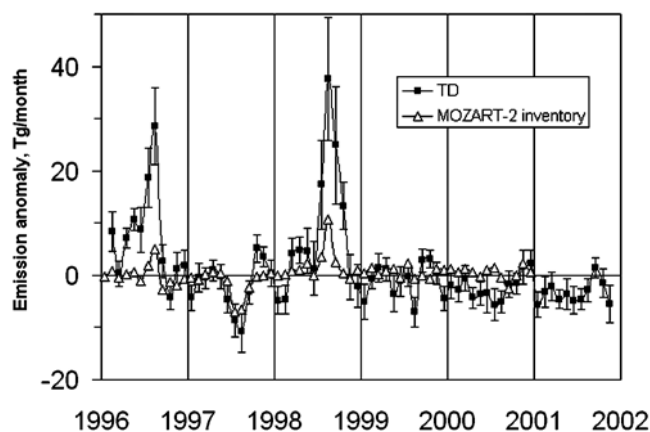


Figure 10. An estimate of anomalies in the surface emission rates for HNH retrieved from the measurements using the box model (top-down (TD) estimate). Error bars correspond to standard error of the anomaly of CO burden (Figure 7). Anomalies of CO surface emission inventory for HNH used in the MOZART-2 chemical transport model are plotted by triangles. See color version of this figure in the HTML.

39 Tg CO per year; catastrophic fires in 1996 and 1998 increased the CO input several times.

[34] In Figure 10 the TD estimate is compared to the surface source anomaly derived from the inventory (“bottom-up”) prepared for the MOZART-2 chemistry transport model [Schultz, 2002; Olivier *et al.*, 1996; M. Schultz and C. Granier, personal communication, 2003]. Seasonality in the CO emissions for particular years was determined by Schultz [2002]. He used a simple scaling approach in order to estimate the variability of biomass burning emissions on the global scale. The method is based on the assumption that the annual totals of the existing inventories [Olivier *et al.*, 1996] represent approximately average conditions and that the seasonal and interannual variability can be introduced by scaling these emissions with some measure of fire activity. The monthly composites of active fire observations from the Along-Track Scanning Radiometer (ATSR) on board the ERS-2 satellite [Arino and Melinotte, 1998] were used as a surrogate for the areas burned (“World Fire Atlas”; <http://shark1.esrin.esa.it/ionia/FIRE/>).

[35] A remarkable agreement in timing of maxima in August 1996 and August 1998 and minimum in August 1997 can be noted. However, the absolute values disagree; for example, there were 38 ± 12 and 11 Tg month⁻¹ in August; 1998 for the top-down and bottom-up estimates, respectively. The reasons for this disagreement and comparisons to other inventories will be discussed below.

5. Discussion

[36] Both the total column measurements and in situ data indicate a significant positive perturbation of the CO balance in summertime of 1998, as well as a buildup in the summertime of 1996. A simple box model was used to estimate monthly mean emission anomalies. The timing of the emission spikes coincides with the months of strong fires; the anomalies of CO emission (Figure 10) were

derived in the MOZART-2 inventory using a climatological mean emissions scaled by fire counts detected by a satelliteborne ATSR. Therefore the seasonality and interannual variations of the MOZART-2 inventory are exclusively based on the measurements of hot spots. This is a strong argument in favor of a leading role for boreal forest fires in the observed anomaly of CO tropospheric burden. However, a large three-fold disagreement in the absolute anomaly of CO emission in Figure 10 requires an explanation. The disagreement may be a result of errors in the parameters of the box model, a misinterpretation of the emission anomalies obtained from the atmospheric CO burden measurements, or errors in the MOZART-2 inventory.

[37] An important factor of uncertainty is the interannual variation of the sink term that has been assumed to be negligible in this paper. Both $\text{TAU}_{\text{trans}}$ and TAU_{chem} were varied in a set of runs (Figure 8), and it was shown that 100% changes in both sink parameters result in only 20–30% of the emission anomaly in August 1998. Unfortunately, it is very difficult to quantify these effects further in the framework of the simple model used.

[38] The fires emit methane and nonmethane hydrocarbons (NMHC) that could be chemically converted to CO. According to Andreae and Merlet [2001], the extratropical forest fires emit (in gram species per kilogram dry matter burned) CO (107), CH₄ (4.7), and total NMHC (5.7). The conversion of methane to CO is too slow to contribute to the CO increase immediately (the chemical lifetime of CH₄ is 8–10 years [Watson *et al.*, 1992]), whereas the atmospheric lifetime of NMHCs can vary from a few hours to several months [Brasseur *et al.*, 1999, p. 346]. For an upper limit of CO converted from NMHC, let us assume that 5.7 g of total NMHC contains 4.9 g of carbon (i.e., similarly to total carbon content for six most abundant hydrocarbons from C₂H₆ to C₃H₈), and this carbon is completely converted in CO. In this case, 11.4 g CO may be added to 107 g CO from 1 kg of dry matter burned. Therefore only 11% of the measured extra CO may be accounted for by conversion from pyrogenic hydrocarbons. One may expect a maximum input of this secondary CO occurring with some delay after the fire events.

[39] There have been several bottom-up estimates of CO released by boreal forest fires in 1998. We can compare our top-down estimate to them if we assume some “normal” (or reference) seasonal cycle of biomass burning emission. Figure 11 presents HNH CO emissions between 1995 and toward the end of 2000, according to the MOZART-2

Table 2. Top-Down Estimates of the CO Emission Anomaly and Total Emission Rates for the Latitudinal Belt 30°N–90°N^a

Year	CO Emission Anomaly, Tg yr ⁻¹	CO Biomass Burning Emission, Tg yr ⁻¹
1996	84 ± 25	136
1997	-23 ± 7	29
1998	96 ± 29	148
1999	-13 ± 4	39
2000	-26 ± 8	26
2001	-37 ± 11	15

^aAbsolute emission rates are given in assumption of the “normal” rates derived in the MOZART-2 inventory that is equal to 52.0 Tg yr⁻¹. Uncertainties of the estimates are standard deviations for eight runs of the box model for perturbed input parameters (see Figure 9).

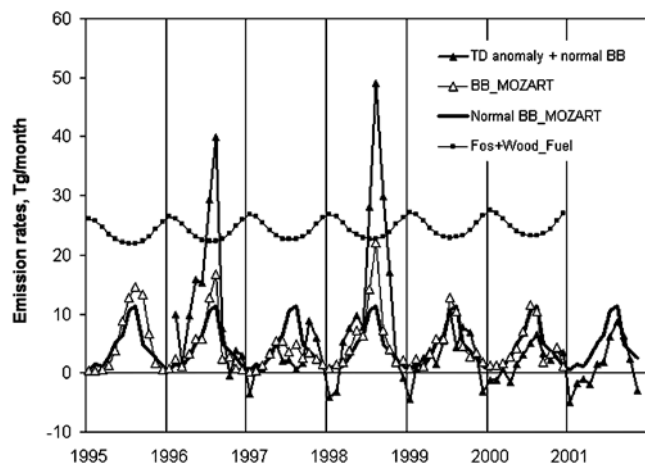


Figure 11. The top-down estimate for the biomass burning emission between 30°N and 90°N (full triangles) in assumption of normal emission rates from the MOZART inventory (solid line). BB is the inventory of biomass burning emission from boreal forest fires, other forest fires, and bush and savanna (steppe) fires. Fos +Wood_Fuel represents CO from combustion of coal, gas, and oil, and their products combined with CO from domestic wood fuel, used for heating and cooking. Normal BB is the average of biomass burning emissions over the period 1995–2000, except 1998. See color version of this figure in the HTML.

inventory [Schultz, 2002; Olivier et al., 1996; M. Schultz and C. Granier, personal communication, 2003]. Also plotted is a curve of biomass emissions averaged over the period from 1995 to 2000, but excepting 1998, and used here as the “normal” seasonal cycle. The emissions retrieved from atmospheric measurements (TD anomaly + normal biomass burning (BB)) in summertime of 1996 and 1998 exceed monthly emissions from fuel combustion. Small negative values in wintertime may be explained either by underestimation of the normal BB or errors in the box model (e.g., in the sink term).

[40] Our top-down “standard” estimate for the monthly mean absolute values of the 1998 biomass CO emissions is plotted in Figure 12 as empty diamonds and a thick line (for $\text{TAU}_{\text{trans}}$ derived from the GEOS-CHEM model and TAU_{chem} according to Spivakovsky et al. [2000]). The error bars take into account the standard errors of the anomaly in CO burden (Figure 6) and the uncertainties of the model (Figure 9), considering them as statistically independent.

[41] The annual 1998 top-down estimate of this paper is compared to available bottom-up estimates (Table 3). Note that these estimates have different geographic extents. Duncan et al. [2003a] calculated total biomass burning for the entire HNH using the ATSR fire counts and aerosol index (AI) from the Total Ozone Mapping Spectrometers (TOMS) data. The K04 estimate includes only the boreal zone, and the KB and Kajii et al. [2002] estimates are only for the Russian boreal forest.

[42] Inventories from MOZART-2 and from three other bottom-up estimates of boreal fire emissions are plotted in Figure 12 (RUS stands for Russia and NA stands for North America). The inventories relied on analysis of AVHRR scenes to determine the total area burned in Russia: Kajii et

al. [2002] estimate $1.1\text{E}7$ ha, Kasischke and Bruhwiler [2002] (KB) estimate $1.31\text{E}7$ ha (derived from Conard et al. [2002]), and Kasischke et al. (submitted manuscript, 2004) (K04) use a figure of $1.15\text{E}7$ ha (A. I. Sukhinin et al., Satellite-based mapping of fires in Russia: New Products for Fire Management and Carbon Cycle Studies, submitted to *Remote Sensing of Environment*, 2004, hereinafter referred to as Sukhinin et al., submitted manuscript, 2004). There are differences between the emission models used for the KB-K04 estimates and that of Kajii et al. [2002], namely:

[43] 1. A higher proportion of crown fires versus ground fires, based on postfire satellite analysis indicating most fires in Siberia are actually crown fires.

[44] 2. Substantial fuel consumption in peatlands.

[45] 3. An explicit increase in fuel consumption in late-season fires, based on field observations and theoretical considerations.

[46] The KB and K04 estimates differ only slightly in the total CO emissions for Russia (the K04 (RUS + NA) estimate also includes CO from North American boreal forest fires) and agree most closely with the magnitude of the top-down estimate. However, there are important differences in the timing of the fire emissions, which result from the use of different data sources for estimating this timing. KB used TOMS aerosol index data as a proxy for fire activity, whereas K04 and Kajii et al. [2002] calculate timing using only hot spot detections from AVHRR. TOMS is not an ideal choice for systematic analysis of fires because the response of the TOMS aerosol index to different parts of the vertical column does not consistently match the vertical distribution of smoke from forest fires. AVHRR hot spots are also an imperfect indicator because they can be foiled by smoke from fires, cloud cover, and other factors (see, e.g., Sukhinin et al., submitted manuscript, 2004). While TOMS indicates that Russian fire activity peaked in September and

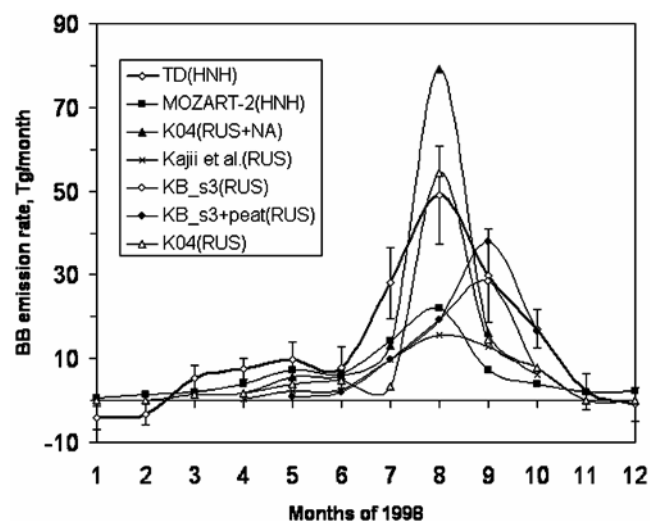


Figure 12. Comparison of the top-down (TD) estimate for CO emission from the biomass burning in 1998 with available inventories. HNH designates all biomass burning between 30°N and 90°N . “RUS” and “NA” correspond to emissions from boreal forest areas in Russia and North America, respectively. For definitions of inventories, see text. See color version of this figure in the HTML.

Table 3. A Comparison of 1998 Top-Down and Bottom-Up (Inventories) Estimates of Biomass Burning CO Emissions in 1998, in Tg CO yr^{-1a}

Source	TD ^b	MOZART-2 Inventory	K04 Inventory	KB With Peat	<i>Kajii et al.</i> [2002]	<i>Duncan et al.</i> [2003a]
Location	HNH	HNH	RUS + NA	only Siberia	only Siberia	HNH
Value	148 ± 30	72	131	86	49	69

^aFor definitions of inventories, see text.

^bMost likely, “normal” is assumed to be 52 Tg yr⁻¹.

October 1998, AVHRR hot spots indicate maximum fire activity in August 1998, with rapidly diminishing activity after that. Neither estimate is a close match to the temporal profile obtained from the top-down result.

[47] The model used in this paper is too simple, and further investigations are needed to improve top-down estimates of CO emission. In particular, a more careful modeling of [OH] and photochemical CO removal are necessary. A detailed modeling of the pyrogenic NMHC chemistry should be performed as well. At this point, however, presented CO totals column measurements and their analysis testify in favor of significant errors in CO emission in 1998 in most of published inventories. This is true both for absolute values (or annual totals) and for timing of CO emission during the year.

6. Conclusions

[48] 1. This paper presents monthly mean total column measurements of carbon monoxide in the high Northern Hemisphere. Anomalies of the total tropospheric CO burden were compared to those derived from in situ measurements. In 1998 and, to a lesser extent, in 1996 the entire middle- to high-latitude belt of the NH experienced a buildup of CO surface concentrations and total column amounts. The maximum enhancement of (40–70)% took place in September–October 1998.

[49] 2. Only at stations in northern Japan did increases of monthly mean CO abundance (both total column and in situ) significantly exceed the hemispheric average. This suggests these stations were directly affected by the westerly transport of Siberian fire emissions. This agrees with the calculations that 70% of wildfire CO emission in 1998 originated in Russia (see Figure 12 and Kasischke et al. (submitted manuscript, 2004)).

[50] 3. A simple box model for the high Northern Hemisphere reservoir was developed, and a top-down estimate for the anomaly of surface emission rates on a monthly basis was obtained. The estimate of the enhanced CO emissions correlates well with the MOZART-2 inventory of CO biomass burning emissions in timing but is much larger in magnitude. Our CO emission estimates for 1998 are comparable only to the highest bottom-up estimates during some months. More careful quantification of the area burned, type and timing of fires, as well as emission factors, may improve the agreement.

Appendix A: Retrieval Algorithms and Locations of the Observational Sites

[51] As indicated in the last column of Table 1, various retrieval algorithms were adopted in the processing of the

observations from the individual sites; a short description for each of these codes is given below. All the analyses relied on spectroscopic parameters compiled in the High-Resolution Transmission (HITRAN-2000) database [*Rothman et al.*, 2003]. More complete information about particular algorithms and their comparisons can be found in the work of *Hase et al.* [2004] and in references given in the following descriptions.

[52] 1. The SFIT2 procedure was jointly developed at the NASA Langley Research Center (LaRC) and at the National Institute of Water and Atmosphere Research (NIWA), Lauder, New Zealand. This algorithm has been described by *Pougatchev et al.* [1995], *Rinsland et al.* [1998, 2000], and *Zhao et al.* [2002]. The vertical mixing ratio profiles of one or two molecules can be retrieved by simultaneously fitting related absorption features in one or more microwindows of the solar spectrum. In this paper, retrievals with SFIT2 were based on three microwindows, i.e., 2057.7–2058.0, 2069.5–2069.8, and 2157.3–2159.2 cm⁻¹. CO total column amounts were calculated by integration over the profiles.

[53] 2. The GFIT algorithm was developed at the Jet Propulsion Laboratory (JPL), Pasadena, California, originally for the fitting of solar absorption spectra recorded from stratospheric balloon platforms and from the Space Shuttleborne Atmospheric Trace Molecule Spectroscopy (ATMOS) instrument. It was modified to work for ground-based measurements of solar absorption spectra. This algorithm fits a calculated spectrum to each observed spectrum in a least squares fashion by scaling the initial mixing ratio profile. The atmosphere is represented as a 100-level model from 0 to 100 km. For each level, line by line calculations are performed to determine the absorption spectrum. GFIT was originally developed for the retrieval of total column densities. The program has been further adapted to retrieve partial columns of three atmospheric layers. Unlike SFIT-2, the modified version of GFIT uses no constraints on the profiles during the analysis; the different altitude layers are treated as independent [*Toon et al.*, 1989; *Notholt et al.*, 2000].

[54] 3. The PROFFIT9 code was developed by *Hase* [2000]. The Rodgers optimal estimation technique is used. The code is capable of handling general covariance matrices. For the efficient construction of simplified empirical covariances, the formalism described by *Tikhonov* [1963] and *Phillips* [1962] is used, enabling the user to apply height-dependent constraints on the variability and the first derivative of the profile with respect to height in each layer. In contrast to the SFIT2, PROFFIT9 does not employ a fixed a priori SNR value of the observed spectrum; it takes this information from the residuals of the fit itself, performing an automatic compensation of quality variations

in the measured spectra. Four microwindows are fitted simultaneously: 2051.2–2051.5, 2057.3–2058.1, 2069.3–2069.9, and 2157.2–2159.1 cm^{-1} .

[55] 4. Total column CO and H₂O amounts were retrieved by least squares fitting of the medium-resolution spectra recorded at Zvenigorod by scaling a priori assumed shapes of vertical mixing ratio profiles [McKernan *et al.*, 1999]. Profile information cannot be retrieved from medium-resolution grating spectra because the fine structure of the spectra, sensitive to the vertical CO distribution, is smoothed by the instrument. A CO a priori profile was taken from Wang *et al.* [1999]. Water vapor a priori profiles (as well as air temperature profiles) were taken from the standard radio soundings made 53 km to the NE of the observational site. Mixing ratio profiles of the interfering gases were assumed from available data corrected for the trend and were not fitted; for CO₂ mixing, the ratio was assumed to be constant at 351 ppm throughout the troposphere. One spectral interval between 2153.7 and 2159.5 cm^{-1} was used. Side-by-side comparisons with FTIRs revealed an agreement to within $\pm 4\%$. A good agreement with CO measured from an aircraft was also obtained. For more details, see Yurganov *et al.* [1999, 2002].

[56] Locations and affiliations of the measurement sites are listed in the Tables 1 and A1. The average numbers of total column observational days per month were between a

Table A1. Surface CO Monitoring Locations

Name	Agency ^a	Latitude	Longitude	Altitude, m
Alert, Nunavut, Canada	CMDL	82.45	−62.50	210
Ny-Alesund, Spitsbergen, Norway	CMDL	78.90	11.88	475
Barrow, Alaska, USA	CMDL	71.32	−56.60	11
“M,” Ocean Station, Norway	CMDL	66.00	2.00	7
Heimaey, Vestmannaeyjar, Iceland	CMDL	63.25	−20.15	100
Shetland Island, UK	CSIRO	60.17	−1.17	30
Cold Bay, Alaska, USA	CMDL	55.20	−62.72	25
Mace Head, Galway, Ireland	CMDL	53.33	−9.90	25
Shemya Island, Alaska, USA	CMDL	52.72	174.10	40
Vancouver, Estavan Pt., BC, Canada	CSIRO	49.38	−26.54	39
Zugspitze, Germany	IMK-IFU	47.42	10.98	2964
Jungfrauoch, Switzerland	EMPA	46.55	7.98	3578
Park Falls, Wisconsin, USA	CMDL	45.93	−90.27	868
Rishiri Island, Japan	NIES	45.07	141.12	35
Ulaan Uul, Mongolia	CMDL	44.45	111.10	914
Sary Taukum, Kazakhstan	CMDL	44.45	77.57	412
Kaz mount, Plateau Assy, Kazakhstan	CMDL	43.25	77.88	2519
Niwot Ridge, Colorado, USA	CMDL	40.05	−05.58	3475
Wendover, Utah, USA	CMDL	39.90	−13.43	1320
Ryori, Japan	JMA	39.03	141.83	230
Azores, Terceira Island, Portugal	CMDL	38.77	−27.38	40
St. Davids, Bermuda, UK	CMDL	32.37	−64.65	30

^aMonitoring agencies are as follows: CMDL, Climate Monitoring and Diagnostics Laboratory, Boulder, Colorado, USA; CSIRO, Commonwealth Science and Industry Research Organization, Canberra, ACT, Australia; JMA, Japan Meteorological Agency, Tokyo, Japan; NIES, National Institute of Environmental Studies, Tsukuba, Japan; IMK-IFU, Forschungszentrum Karlsruhe, Garmisch-Partenkirchen, Germany; EMPA, Swiss Federal Laboratories for Materials Testing and Research, St. Gallen, Switzerland. The measurements at Rishiri Island, Ryori, and Zugspitze were carried out continuously; weekly sampling with following analysis in a laboratory was used at other sites.

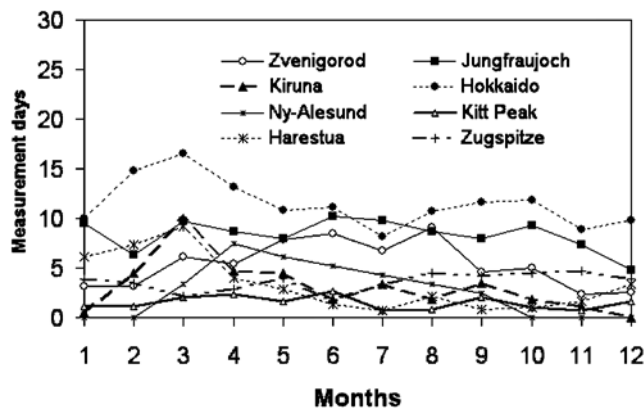


Figure A1. Numbers of measurement days per month averaged for 1996–2001. See color version of this figure in the HTML.

few and 15 (Figure A1). Weekly sampling was used at the most of sites but two; at Rishiri Island and at Ryori the measurements were continuous.

[57] **Acknowledgments.** The authors thank M. Schultz and C. Granier for providing the MOZART-2 inventory of CO sources. T.B., F.H., V.V., A.S., J.N., and J.M. like to thank for funding from the Bundesministerium für Bildung und Forschung via the DLR by contracts 50EE0008 and 50EE0203 and from the European Union within the UFTIR project (EVK2-2002-00159). T.B. and F.H. are grateful to the colleagues at IRF for their support and to the Goddard Space Flight Center for providing the temperature and pressure profiles of the National Centers for Environmental Prediction used for inversion. V.V., A.S., and J.N. acknowledge the financial support provided by the European Union within SOGE and national funding for SCIAMACHY validation. E. I.G. and L.N.Y. thank A.V. Dzholia for making measurements and analysis; they acknowledge a financial support from the Russian Fund for Basic Research (grant RFBR 02-05-64148). L.N.Y. is grateful to H. Akimoto for his interest and helpful discussions. C.P.R. was supported by NASA’s Upper Atmosphere Research Program and the Atmospheric Chemistry Modeling and Analysis Program. Work performed at the University of Liège and at the Jungfrauoch (R.Z. and E.M.) was primarily supported by Belgian (OSTC) and EC funds. A.S. and J.M. acknowledge the financial support provided by the Swedish National Space Board. Funding of the activities at the Zugspitze observatory by German BMBF and the EC is gratefully acknowledged by R.S. The authors are grateful to O. Wild for editing style and grammar.

References

- Andreae, M. O., and P. Merlet (2001), Emission of trace gases and aerosols from biomass burning, *Global Biogeochem. Cycles*, 15(4), 955–966.
- Ariño, O., and J. Melinotte (1998), The 1993 Africa fire map, *Int. J. Remote Sens.*, 19, 2019–2023.
- Bey, I., D. J. Jacob, R. M. Yantosca, J. A. Logan, B. D. Field, A. M. Fiore, Q. Li, H. Liu, L. J. Mickley, and M. Schultz (2001), Global modeling of tropospheric chemistry with assimilated meteorology: Model description and evaluation, *J. Geophys. Res.*, 106, 23,073–23,095.
- Brasseur, G., J. Orlando, and G. Tyndall (Eds.) (1999), *Atmospheric Chemistry and Global Change*, 360 pp., Oxford Univ. Press, New York.
- Conard, S. G., A. L. Sukhinin, B. J. Stocks, D. R. Cahoon, D. P. Davidenko, and G. A. Ivanova (2002), Determining effects of area burned and fire severity on carbon cycling and emissions in Siberia, *Clim. Change*, 55(1–2), 197–211.
- Daniel, J. S., and S. Solomon (1998), On the climate forcing of carbon monoxide, *J. Geophys. Res.*, 103, 13,249–13,260.
- DeMore, W. B., S. P. Sander, D. M. Golden, R. F. Hampson, M. J. Kurylo, C. J. Howard, A. R. Ravishankara, C. E. Kolb, and M. J. Molina (1997), Chemical kinetics and photochemical data for use in stratospheric modeling, *JPL Publ.* 97-4.
- Duncan, B. N., R. V. Martin, A. C. Staudt, R. Yevich, and J. A. Logan (2003a), Interannual and seasonal variability of biomass burning emissions constrained by satellite observations, *J. Geophys. Res.*, 108(D2), 4100, doi:10.1029/2002JD002378.
- Duncan, B. N., I. Bey, M. Chin, L. J. Mickley, T. D. Fairlie, R. V. Martin, and H. Matsueda (2003b), Indonesian wildfires of 1997; Impact on tropo-

- spheric chemistry, *J. Geophys. Res.*, 108(D15), 4458, doi:10.1029/2002JD003195.
- Ehhalt, D., et al. (2001), Atmospheric chemistry and greenhouse gases, in *Climate Change 2001: The Scientific Basis, Contribution of Working Group I to the Third Assessment Report of the Intergovernmental Panel on Climate Change*, edited by J. T. Houghton et al., chap. 4, pp. 241–287, Cambridge Univ. Press, New York.
- Forster, C., et al. (2001), Transport of boreal forest fire emissions from Canada to Europe, *J. Geophys. Res.*, 106(D19), 22,887–22,906.
- Hase, F. (2000), Retrieval of trace gas profiles from high resolution ground-based FTIR measurements, *FZK Rep. 6512*, Forschungszentrum Karlsruhe, Karlsruhe.
- Hase, F., J. W. Hannigan, M. T. Coffey, A. Goldman, M. Höpfner, N. B. Jones, C. P. Rinsland, and S. W. Wood (2004), Intercomparison of retrieval codes used for the analysis of high-resolution, ground-based FTIR measurements, *J. Quant. Spectrosc. Radiat. Transfer*, 87(1), 25–52.
- Holloway, T., H. Levy II, and P. Kasibhatla (2000), Global distribution of carbon monoxide, *J. Geophys. Res.*, 105, 12,123–12,147.
- Kajii, Y., et al. (2002), Boreal forest fires in Siberia in 1998: Estimation of area burned and emissions of pollutants by advanced very high resolution radiometer satellite data, *J. Geophys. Res.*, 107(D24), 4745, doi:10.1029/2001JD001078.
- Kasischke, E. S., and L. P. Bruhwiler (2002), Emissions of carbon dioxide, carbon monoxide, and methane from boreal forest fires in 1998, *J. Geophys. Res.*, 107, 8146, doi:10.1029/2001JD000461 [printed 108(D1), 2003].
- Logan, J. A., M. J. Prather, S. C. Wofsy, and M. B. McElroy (1981), Tropospheric chemistry: A global perspective, *J. Geophys. Res.*, 86, 7210–7254.
- McKernan, E., L. N. Yurganov, B. T. Tolton, and J. R. Drummond (1999), MOPITT validation using ground-based IR spectroscopy, *Proc. SPIE*, 3756, 486–491.
- Minzner, R. A. (1977), The 1976 standard atmosphere and its relationship to earlier standards, *Rev. Geophys.*, 15, 375–384.
- Notholt, J., G. C. Toon, C. P. Rinsland, N. S. Pougatchev, N. B. Jones, B. J. Connor, R. Weller, M. Gautrois, and O. Schrems (2000), Latitudinal variations of trace gas concentrations in the free troposphere measured by solar absorption spectroscopy during a ship cruise, *J. Geophys. Res.*, 105(D1), 1337–1349.
- Novelli, P. C., K. A. Masarie, and P. M. Lang (1998), Distributions and recent changes of carbon monoxide in the lower troposphere, *J. Geophys. Res.*, 103, 19,015–19,033.
- Novelli, P. C., K. A. Masarie, P. M. Lang, B. D. Hall, R. C. Myers, and J. W. Elkins (2003), Reanalysis of tropospheric CO trends: Effects of the 1997–1998 wildfires, *J. Geophys. Res.*, 108(D15), 4464, doi:10.1029/2002JD003031.
- Olivier, J., A. Bouwman, C. van der Maas, J. Berdowski, C. Veldt, J. Bloos, A. Visschedijk, P. Zandveld, and J. Haverlag (1996), Description of EDGAR Version 2.0: A set of global emission inventories of greenhouse gases and ozone-depleting substances for all anthropogenic and most natural sources on a per country basis and on 1×1 grid, *Tech. Rep. 771060 002*, Nat. Inst. of Public Health and the Environ., Bilthoven.
- Phillips, D. (1962), A technique for the numerical solution of certain integral equations of the first kind, *J. Assoc. Comput. Math.*, 9, 84–97.
- Pougatchev, N. S., B. J. Connor, and C. P. Rinsland (1995), Infrared measurements of the ozone vertical distribution above Kitt Peak, *J. Geophys. Res.*, 100, 16,689–16,697.
- Rinsland, C. P., et al. (1998), Northern and Southern Hemisphere ground-based infrared spectroscopic measurements of tropospheric carbon monoxide and ethane, *J. Geophys. Res.*, 103, 28,197–28,217.
- Rinsland, C. P., et al. (1999), Infrared solar spectroscopic measurements of free tropospheric CO, C₂H₆, and HCN above Mauna Loa, Hawaii: Seasonal variations and evidence for enhanced emissions from the southeast Asian tropical fires of 1997–1998, *J. Geophys. Res.*, 104, 18,667–18,680.
- Rinsland, C. P., E. Mahieu, R. Zander, P. Demoulin, J. Forrer, and B. Buchmann (2000), Free tropospheric CO, C₂H₆, and HCN above center Europe: Recent measurements from the Jungfraujoch station including the detection of elevated columns during 1998, *J. Geophys. Res.*, 105, 24,235–24,249.
- Rothman, L. S., et al. (2003), The HITRAN molecular spectroscopic database: Edition of 2000 including updates through 2001, *J. Quant. Spectrosc. Radiat. Transfer*, 82, 5–44.
- Schultz, M. G. (2002), On the use of ATSR fire count data to estimate the seasonal and interannual variability of vegetation fire emissions, *Atmos. Chem. Phys.*, 2, 387–395.
- Seiler, W. (1974), The cycle of atmospheric CO, *Tellus*, 26, 116–135.
- Spivakovsky, C. M., et al. (2000), Three-dimensional climatological distribution of tropospheric OH: Update and evaluation, *J. Geophys. Res.*, 105, 8931–8980.
- Taguchi, S., H. Matsueda, H. Y. Inoue, and Y. Sawa (2002), Long range transport of carbon monoxide from tropical ground to upper troposphere: A case study for southeast Asia in October, 1997, *Tellus, Ser. B*, 54, 22–44.
- Tanimoto, H., Y. Kajii, J. Hirokawa, H. Akimoto, and N. Minko (2000), The atmospheric impact of boreal forest fires in far eastern Siberia on the seasonal variation of carbon monoxide: Observations at Rishiri, a northern remote island in Japan, *Geophys. Res. Lett.*, 27, 4073–4076.
- Tikhonov, A. N. (1963), On the solution of incorrectly stated problems and a method of regularization, *Dokl. Akad. Nauk SSSR*, 151, 501–506.
- Toon, G. C., C. B. Farmer, P. W. Schaper, J. F. Blavier, and L. L. Lowes (1989), Ground based infrared measurements of tropospheric source gases over Antarctica during the 1986 austral spring, *J. Geophys. Res.*, 94(D9), 1613–1624.
- TRACE-P Science Team (2003), Preface to the NASA Global Tropospheric Experiment Transport and Chemical Evolution Over the Pacific (TRACE-P): Measurements and analysis, *J. Geophys. Res.*, 108(D20), 8780, doi:10.1029/2003JD003851.
- van der Werf, G. R., J. T. Randerson, G. J. Collatz, L. Giglio, P. S. Kasibhatla, A. F. Arellano Jr., S. C. Olsen, and E. S. Kasischke (2004), Continental-scale partitioning of fire emissions during the 1997 to 2001 El Niño/La Niña period, *Science*, 303(5654), 73–76.
- Wang, J., M. N. Deeter, J. C. Gille, and P. L. Bailey (1999), Retrieval of tropospheric carbon monoxide profiles from MOPITT: Algorithm description and retrieval simulation, *Proc. SPIE*, 3756, 455–465.
- Watson, R. T., L. G. Meiro Filho, E. Sanhueza, and A. Janetos (1992), Greenhouse gases: Sources and sinks, in *Climate Change 1992: The Supplementary Report to the IPCC Scientific Assessment*, edited by J. T. Houghton, B. A. Callander, and S. K. Varney, Cambridge Univ. Press, New York.
- World Meteorological Organization (WMO) (2003), *WDCGG Data Summary: GAW Data*, vol. IV, *Greenhouse Gases and Other Atmospheric Gases*, WDCGG 27, Geneva.
- Wotawa, G., P. C. Novelli, M. Trainer, and C. Granier (2001), Interannual variability of summertime CO concentrations in the Northern Hemisphere explained by boreal forest fires in North America and Russia, *Geophys. Res. Lett.*, 24, 4575–4578.
- Yurganov, L. N., E. I. Grechko, and A. V. Dzhola (1999), Zvenigorod carbon monoxide total column time series: 27 yr of measurements, *Chem. Global Change Sci.*, 1, 127–136.
- Yurganov, L. N., E. I. Grechko, and A. V. Dzhola (2002), Long-term measurements of carbon monoxide over Russia using a spectrometer of medium resolution, *Recent Res. Devel. Geophys.*, 4, 249–265.
- Zhao, Y., et al. (2002), Spectroscopic measurements of tropospheric CO, C₂H₆, C₂H₂, and HCN in northern Japan, *J. Geophys. Res.*, 107(D18), 4343, doi:10.1029/2001JD000748.
- T. Blumenstock, F. Hase, and I. Kramer, IMK-ISF, Forschungszentrum Karlsruhe, Postfach 3640, Karlsruhe D-76021, Germany.
- E. I. Grechko, Obukhov Institute of Atmospheric Physics, 3 Pyzhevsky Per., Moscow 109017, Russia.
- E. J. Hyer and E. S. Kasischke, Department of Geography, University of Maryland, 2181 LeFrak Hall, College Park, MD 20742, USA.
- M. Koike and Y. Kondo, University of Tokyo, 7-3-1 Hongo, Bunkyo, Tokyo 113-0033, Japan.
- F.-Y. Leung, Division of Engineering and Applied Sciences, Department of Earth and Planetary Sciences, Harvard University, Cambridge, MA 02138, USA.
- E. Mahieu and R. Zander, Institute of Astrophysics and Geophysics, University of Liège, Liège B-4000, Belgium.
- J. Mellqvist and A. Strandberg, Radio and Space Science, Chalmers University of Technology, Göteborg S-41296, Sweden.
- J. Notholt, University of Bremen, Bremen D-28359, Germany.
- P. C. Novelli, Climate Monitoring and Diagnostic Laboratory, NOAA, 325 Broadway, Boulder, CO 80303, USA.
- C. P. Rinsland, Atmospheric Sciences Division, NASA Langley Research Center, Mail Stop 401A, 21 Langley Blvd., Hampton, VA 23681-0001, USA.
- H. E. Scheel and R. Sussmann, IMK-IFU, Forschungszentrum Karlsruhe, Kreuzackbahnstrasse 19, Garmisch-Partenkirchen D-82467, Germany.
- A. Schulz, Alfred-Wegener-Institute, Potsdam D-14473, Germany.
- H. Tanimoto, National Institute for Environmental Studies, 16-2 Onogawa, Tsukuba 305-8506, Japan.
- V. Velazco, University of Bremen, Otto Hahn Allee 1, Bremen D-28359, Germany.
- L. N. Yurganov, Frontier Research System for Global Change, Japan Agency for Marine-Earth Science and Technology, 3173-25 Showa-machi, Yokohama 236-0001, Japan. (leonid@jamstec.go.jp)
- Y. Zhao, University of California, 1 Shields Avenue, Davis, CA 95616, USA.